THE JOURNAL OF BIOLOGICAL CHEMISTRY
Vol. 278, No. 36, Issue of September 5, pp. 34119–34124, 2003
Printed in U.S.A.


# Endoplasmic Reticulum-associated Degradation of Mammalian Glycoproteins Involves Sugar Chain Trimming to $Man_{6-5}GlcNAc_2$*

Received for publication, June 5, 2003, and in revised form, June 19, 2003
Published, JBC Papers in Press, June 26, 2003, DOI 10.1074/jbc.M305929200

**Zehavit Frenkel‡, Walter Gregory§, Stuart Kornfeld§, and Gerardo Z. Lederkremer‡¶**

*From the ‡Department of Cell Research and Immunology, George Wise Faculty of Life Sciences, Tel Aviv University, Tel Aviv 69978, Israel and §Division of Hematology, Washington University School of Medicine, St. Louis, Missouri 63110*

**Endoplasmic reticulum-associated degradation of misfolded or misprocessed glycoproteins in mammalian cells is prevented by inhibitors of class I α-mannosidases implicating mannose trimming from the precursor oligosaccharide $Glc_3Man_9GlcNAc_2$ as an essential step in this pathway. However, the extent of mannose removal has not been determined. We show here that glycoproteins subject to endoplasmic reticulum-associated degradation undergo reglucosylation, deglucosylation, and mannose trimming to yield $Man_6GlcNAc_2$ and $Man_5GlcNAc_2$. These structures lack the mannose residue that is the acceptor of glucose transferred by UDP-Glc:glycoprotein glucosyltransferase. This could serve as a mechanism for removal of the glycoproteins from folding attempts catalyzed by cycles of reglucosylation and calnexin/calreticulin binding and result in targeting of these molecules for proteasomal degradation.**

Trimming of the asparagine-linked precursor oligosaccharide $Glc_3Man_9GlcNAc_2$ in the endoplasmic reticulum (ER)[1] yields $Glc_1Man_{9-7}GlcNAc_2$ (G1M9–7) that associates with the ER chaperones/lectins calnexin (CNX) and calreticulin (CRT) (1). A folding and quality control process is then initiated that consists of cycles of deglucosylation by glucosidase II, release from the chaperone, reglucosylation by the folding sensor enzyme UDP-Glc:glycoprotein glucosyltransferase (GT), and reassociation with CNX and CRT (2). Glycoproteins that achieve proper folding are no longer recognized by GT and leave this cycle.

Trimming of mannose (Man) residues is involved in the disposal of ER-retained glycoproteins that cannot be driven to their native forms during the cycles of binding to CNX/CRT (3). It was proposed that Man trimming may provide a timer that allows these folding attempts before degradation starts (3, 4). Thus, inhibitors that prevent Man trimming were found to inhibit the ERAD of many defective glycoproteins (4–8). In the absence of these inhibitors, the glycoproteins are ubiquitinated and delivered to the cytosolic proteasomes for degradation (9). Prior to dislocation to the cytosol, the substrates are transported to a specialized compartment termed the quality control (QC) compartment together with CNX and CRT (10). This compartment is pericentriolar, located near (but not overlapping) the Golgi and the ER-Golgi intermediate compartment (ERGIC), and is dependent on microtubules.

Whereas the inhibitor studies provide strong evidence that Man trimming is involved in ERAD, the structures of the *N*-linked oligosaccharides that result from trimming have not been determined in mammalian cells. The inhibitors that prevent Man trimming leading to ERAD (such as 1-deoxymannojirimycin (dMNJ) and kifunensine) are blockers of class I mannosidases. Therefore, the major ER class I enzyme, ER mannosidase I, has been proposed to be responsible for this pathway. Consequently, the product of cleavage by this enzyme, an M8 isomer lacking the middle branch terminal Man (M8B), has been suggested as the signal that marks the glycoprotein for ERAD (4). However, glycoproteins that exit the ER toward the Golgi can undergo trimming to M8B with no detectable effect. Therefore, we set out to characterize the structures of the *N*-linked oligosaccharides that are the product of Man trimming leading to ERAD and to determine the effect of this trimming in glycoprotein localization and interactions with CNX. Here we show for known ERAD substrates, the uncleaved precursor of asialoglycoprotein receptor (ASGPR) H2a (a type II transmembrane glycoprotein), its soluble cleaved 35-kDa luminal fragment, and unassembled CD3 δ (a type I transmembrane glycoprotein), that Man trimming yields $Man_6GlcNAc_2$ (M6) and $Man_5GlcNAc_2$ (M5) oligosaccharides. These species lack the Man residue that is the acceptor for Glc transfer and thus provide a mechanism for these glycoproteins to escape from the reglucosylation cycle. Absent reglucosylation, these glycoproteins can enter the ERAD pathway.

## EXPERIMENTAL PROCEDURES

*Materials*—Rainbow $^{14}C$-labeled methylated protein standards were obtained from Amersham Biosciences. Pro-mix cell labeling mixtures ([$^{35}S$]Met plus [$^{35}S$]Cys, >1000 Ci/mmol) and Man (D-[2-$^3H$(N)], 21 Ci/mmol) were from PerkinElmer Life Sciences. Protein A-Sepharose was from Repligen (Needham, MA). Endo-*N*-acetylglucosaminidase H (endo H) was obtained from New England Biolabs (Beverly, MA), and castanospermine (CST) was from Genzyme Corp. (Boston, MA). Lactacystin (Lac), *N*-carbobenzoxyl-leucinyl-leucinyl-leucinal (MG-132), and dMNJ were from Calbiochem (La Jolla, CA). Jack bean α-mannosidase and other common reagents were from Sigma.

*Cells and Culture*—NIH 3T3 fibroblasts expressing H2a (2–18 cells) (11), H2a with a mutated cleavage site, G78R, (AGR-1 cells) (12), and the ER-retained H1 mutant, H1i5 (5D cells) (13), were grown in Dulbecco's modified Eagle's medium plus 10% newborn calf serum under 5% $CO_2$ at 37 °C. COS-7 cells were grown similarly but with 10% fetal calf serum. Plasmid pCDδM containing CD3δ was transfected into COS-7 cells in 35-mm dishes using the FuGENE 6 transfection reagent (Roche Applied Science) according to the provided protocol.

*Antibodies*—Polyclonal anti-C-terminal antibodies against H1 (αH1) or H2 (αH2) were the ones used in earlier studies (13). R9, anti-C-terminal CD3δ polyclonal was a kind gift from L. Samelson (NCI,

* This work was supported by a grant from the United States-Israel Binational Science Foundation and a grant from the Israel Science Foundation (to G. Z. L.), founded by the Israeli Academy of Sciences.

¶ To whom correspondence should be addressed. Tel.: 972-3-640-9239; Fax: 972-3-642-2046; E-mail: gerardo@post.tau.ac.il.

[1] The abbreviations used are: ER, endoplasmic reticulum; ERAD, endoplasmic reticulum-associated degradation; CNX, calnexin; CRT, calreticulin; GT, UDP-Glc:glycoprotein glucosyltransferase; QC, quality control; IP, immunoprecipitation; ASGPR, asialoglycoprotein receptor; endo H, endo-*N*-acetylglucosaminidase H; MG-132, *N*-carbobenzoxyl-leucinyl-leucinyl-leucinal; Lac, lactacystin; CST, castanospermine; dMNJ, 1-deoxymannojirimycin; EDEM, ER-degradation enhancing α mannosidase-like protein; G3M9–M5, $Glc_3Man_9GlcNAc_2$-$Man_5GlcNAc_2$; ERGIC, ER-Golgi intermediate compartment.

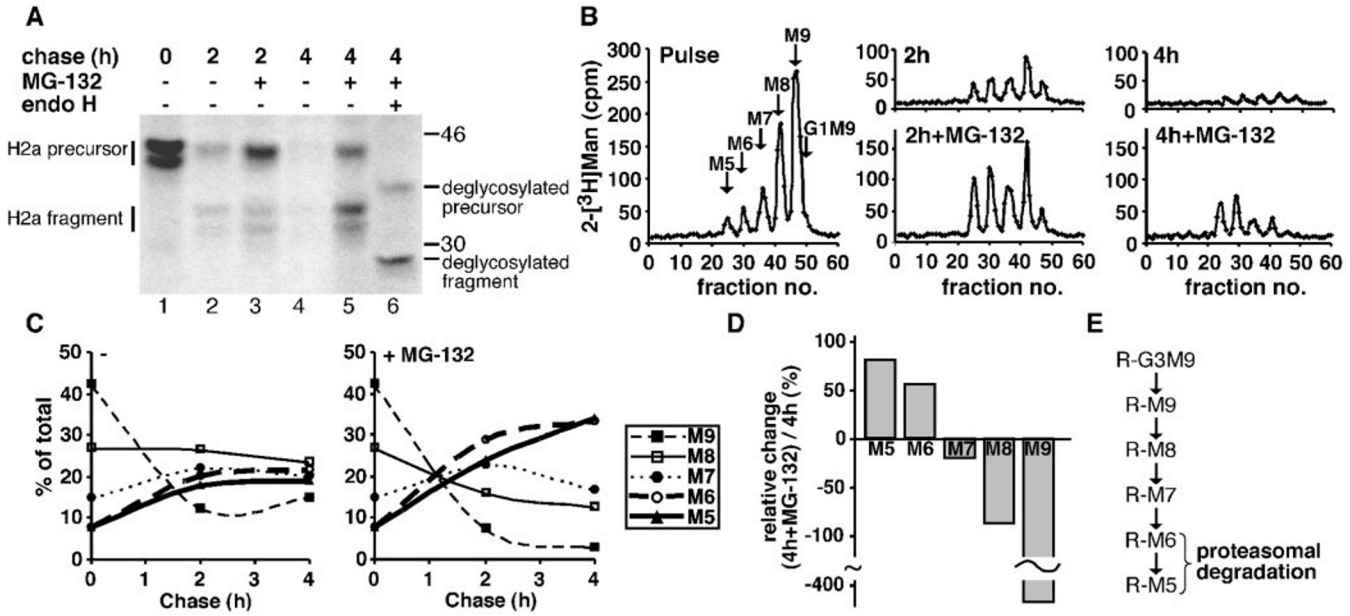


FIG. 1. **Accumulation of M6 and M5 *N*-linked oligosaccharides on ASGPR H2a upon proteasomal inhibition.** *A*, NIH 3T3 cells stably expressing H2a (2–18 cell line) were metabolically labeled with [$^{35}$S]Cys for 20 min and chased with complete medium in the absence or presence of 20 $\mu$M MG-132. Cells were lysed, and H2a was immunoprecipitated, treated in one case (*lane 6*) with endo H, and run on SDS-PAGE followed by fluorography. *Bands* corresponding to the H2a precursor and the naturally occurring cleaved fragment are indicated on the *left*. Molecular mass markers in kilodaltons are indicated on the *right*. *B*, the same cells as in *A* were labeled with [2-$^3$H]Man for 1 h in a Glc-free medium and chased for the indicated times in complete medium in the absence or presence of 20 $\mu$M MG-132. *N*-Linked oligosaccharides separated with endo H from H2a immunoprecipitates were analyzed by high pressure liquid chromatography, and fractions were counted in a beta counter. Counts per min of a representative experiment of three repeat experiments are presented as a function of the fraction number. M5–M9 and *G1M9* indicate the migration of oligosaccharide standards. *C*, relative molar amounts of each oligosaccharide species in *B* were calculated based on Man content. The percent of each species relative to the total sum of the molar amounts of all species present was then plotted as a function of chase time. *D*, the plot shows the percent of relative increase in the presence of MG-132 compared with the absence, which was calculated by dividing the values of percent of the total of each species (from *C*) at a chase time of 4 h with MG-132 by those without MG-132, subtracting 1, and multiplying by 100 (*e.g.* for M5 there is 1.8-fold increase that translates in the graph to an 80% increase). For decreases, the same calculation was done, but values without MG-132 were divided by those with the inhibitor; a *negative sign* was added to signify a decrease. *E*, a scheme of the Glc and Man trimming processes that would lead to M6 and M5 linked to a protein (*R*) that is targeted to ERAD.

National Institutes of Health, Bethesda, MD). Polyclonal anti-calnexin was from Stressgen Biotechnologies Corp. (Victoria, British Columbia, Canada) and mouse monoclonal anti-$\beta$-COP from Sigma. Goat anti-rabbit antibody conjugated to Cy3 (indocarbocyanine) and goat anti-mouse antibody conjugated to fluorescein isothiocyanate were from Jackson Laboratories (West Grove, PA).

*[$^{35}$S]Cys Metabolic Labeling and Immunoprecipitation*—For stable cell lines, subconfluent (90%) cell monolayers in 60-mm dishes were labeled with [$^{35}$S]Cys, lysed, and immunoprecipitation (IP) was done as described previously with anti-H2 antibody (13, 14). For transiently transfected CD3$\delta$, similar conditions were used except that labeling was done in 35-mm dishes 2 days after transfection with 160 $\mu$Ci/ml [$^{35}$S]Cys plus [$^{35}$S]Met mix. CST (150 $\mu$g/ml), or the proteasome inhibitors MG-132 (20 $\mu$M), or Lac (10 $\mu$M) were added to the chase medium. Treatments with endo H or jack bean $\alpha$-mannosidase after IP and analysis of association with calnexin were performed as described previously (13).

*Gel Electrophoresis, Fluorography, and Quantitation*—Reducing SDS-PAGE was performed on 10% Laemmli gels. The gels were analyzed by fluorography using 20% 2,5-diphenyloxazole and were exposed to Kodak BioMax MR film, except for the calnexin co-IP experiment where Biomax MS film and a transcreen-LE from Kodak were used. Quantitation was performed in a Fuji BAS 2000 phosphorimaging device.

*[2-$^3$H]Man Labeling and Analysis of N-linked Oligosaccharides*—For stable cell lines, subconfluent (90%) monolayers of cells in 100-mm tissue culture dishes were rinsed and preincubated for 30 min at 37 °C with Glc-free Dulbecco's modified Eagle's medium plus 10% dialyzed calf serum. They were then pulse-labeled for 30–60 min in the same medium containing 400 $\mu$Ci/ml [2-$^3$H]Man. Labeling of transiently transfected CD3$\delta$ was similar except in 35-mm dishes with 240 $\mu$Ci/ml [2-$^3$H]Man. Cells were rinsed and chased with normal Dulbecco's modified Eagle's medium plus 10% calf serum. Cell lysis, IP, and endo-H treatment were performed as described for $^{35}$S-labeled samples. Samples were then filtered on a Centricon 30 (for H2a, H1i5, and G78R) or a Centricon 10 (for CD3$\delta$). Elution was done three times with 100 $\mu$l of $H_2O$ each time. The flow-through containing high mannose *N*-linked oligosaccharides was analyzed by high pressure liquid chromatography according to the procedure described in Ref. 15.

*Immunofluorescence Microscopy*—The procedures employed were as described previously (10, 13). For treatments with Lac (10 $\mu$M) or dMNJ (75 $\mu$g/ml), cells on coverslips were incubated with medium containing the drug at 37 °C in a $CO_2$ incubator for 5 h. Digital photography on a Leica DMRBE fluorescence microscope was done at identical exposure times between samples so that signal intensities could be compared.

## RESULTS

*Mannose Trimming to M6 and M5 on an ERAD Substrate, ASGPR H2a*—We studied ASGPR H2a as a model ERAD substrate glycoprotein. During its normal expression in hepatocytes, H2a is efficiently secreted as a soluble form of the receptor (14). Although the H2a precursor is a type II membrane protein, the evidence suggests that it is cleaved by signal peptidase in the ER releasing its ectodomain (12). When transfected into other cell types (such as fibroblasts), the efficiency of this process is much reduced, many precursor molecules remain uncleaved, are retained in the ER, and are sent to ERAD (10, 11). The uncleaved precursors contain an ER retention signal that prevents them from exiting to the Golgi (13). For the molecules that are cleaved in fibroblasts, a portion of the soluble fragment is secreted, but most is also degraded by ERAD (10, 14). A pulse-chase analysis with [$^{35}$S]Cys of H2a that is stably expressed in NIH 3T3 cells shows degradation of the membrane-bound precursor (Fig. 1*A*). This degradation was inhibited by MG-132 and other proteasomal inhibitors (Fig. 1*A* and Ref. 10). Although the *N*-glycans on the secreted fragment are processed to complex type species in the Golgi, intracellular molecules are always sensitive to endo H (Fig. 1*A*, *lane 6*),

suggesting a fast transit through the Golgi of molecules that are not sent to ERAD. The lower band in Fig. 1*A*, *lane 1,* represents precursor molecules that are underglycosylated (one of the three possible *N*-glycosylation sites is not utilized).[2] The small shift to a faster mobility seen after the chase (Fig. 1*A*, compare *lanes 1–3*) is because of Man trimming. Both the trimming and the degradation of H2a are blocked by the mannosidase inhibitor dMNJ (6).

To analyze the *N*-linked glycans on H2a, the cells were metabolically labeled with [2-$^3$H]Man followed by lysis, IP of H2a, and release of its high mannose oligosaccharides with endo H. Less than 1% of the label was resistant to endo H. High pressure liquid chromatography separation yielded species from the pulse sample that co-migrated with M9, M8, M7, M6, and M5 standards in decreasing amounts (Fig. 1*B*, *upper left panel*). A small amount of G1M9 and G1M8 was also present as further analysis of the M9 peak indicated. After 2 h of chase, the amounts of the larger species decreased, whereas those of the smaller species increased. This was more prominent when the cells were incubated with MG-132, especially after 4 h of chase (Fig. 1*B*, *lower right panel*). M6 and M5, the result of the Man-trimming process, increased after 2 h of chase in the presence or absence of MG-132, and after 4 h they disappeared because of degradation of H2a, but proteasomal inhibition led to their accumulation.

When the data are expressed as the percent of each oligosaccharide species compared with all species on a molar basis, the processing of M9 and M8 to M6 and M5 is clear, especially in the presence of MG-132 (Fig. 1*C*). M7 is a typical intermediate with a transient increase after 2 h and then a decrease after 4 h of chase (Fig. 1*C*, *right panel*). Fig. 1*D* shows a relative increase at the end of the chase period in M6 and M5 when samples with and without proteasomal inhibition are compared. In contrast, there is a relative decrease in M8 and M9 and a small decrease in M7. The results are consistent with the protein molecules bearing M6 and M5 after Man trimming being the ones targeted to proteasomal degradation (Fig. 1*E*). A similar experiment performed in the presence of the proteasomal inhibitor Lac yielded comparable results (Fig. 2, *A–C*). In this experiment, a shorter chase of 1 h was included enabling observation of the change in the pattern of oligosaccharide species before the end of a lag that precedes the start of degradation (11). Fig. 2*B* shows that after a 1-h chase, there is very little difference between the patterns in the presence or absence of Lac, with an increase in the relative amount of M6 and M5 already evident (Fig. 2*B*). This increase in M6 and M5, after only a 1-h chase and even in the absence of Lac, indicates that the extensive trimming is not the result of the proteasomal inhibition or of long retention in the ER.

As described above, H2a precursor is cleaved to a 35-kDa luminal fragment. To exclude the possibility that we were mostly examining the trimming of sugar chains on this fragment, we studied a mutant of H2a (G78R) that has the cleavage site mutated. This mutant is completely retained and degraded at a rate similar to wild-type H2a (12). The results obtained were similar to those with wild-type H2a with a relative increase in M6 and M5, although the low efficiency of the labeling allowed us to follow the course for only 2 h of chase, resulting in a lower accumulation of these glycans (Fig. 2*D*).

*Mannose Trimming to M6 and M5 Depends on the Degree of Instability of the Glycoprotein and Not on Its ER Retention*—We next examined a glycoprotein that is retained in the ER but is much more stable than H2a to determine whether Man trimming to M6 and M5 can arise from ER retention unrelated to

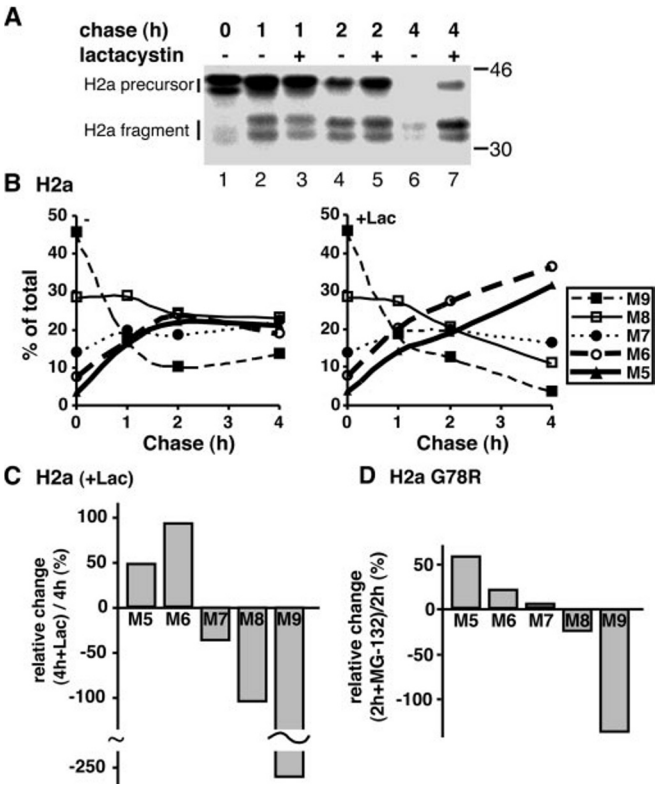


FIG. 2. **Man trimming to M6 and M5 is observable before the start of proteasomal degradation; similar trimming of an uncleavable H2a mutant.** *A–C*, similar to Fig. 1, but in this case the cells were labeled for 30 min and the proteasomal inhibitor Lac (10 $\mu$M) was used instead of MG-132. A shorter chase time point of 1 h was included, which is when the ERAD process starts to emerge from a lag before degradation of H2a begins. *D*, similar to Fig. 1*D,* but in this case the experiment was done with NIH 3T3 cells expressing the ASGPR H2a mutant G78R, which has identical instability as H2a and is an ERAD substrate but does not produce a cleavage fragment.

proteasomal degradation. H1i5 is a mutant of the ASGPR H1 subunit that is completely retained in the ER but with a half-life of about 8 h as compared with 1 h for H2a. The retention was achieved by the introduction of the pentapeptide EGHRG from the juxtamembrane luminal region of H2a that acts as a retention signal (13). H1i5 glycans were processed similarly in the presence and absence of MG-132, with a rate of trimming to M8 and M7 similar to H2a but much slower trimming to M6 and M5 (Fig. 3*A*, compare with Fig. 1*C*). After a 4-h chase, H1i5 showed no preferential accumulation of M6 and M5 (Fig. 3*B*). This result suggests that the trimming to M6 and M5 is directly related to the instability of the glycoprotein and not to its ER retention. The process cannot simply depend on the time of ER residence; rather, it involves specific recognition of the ERAD substrate by the mannosidase. Alternatively, the ERAD substrate may be targeted to a compartment where the mannosidase resides.

To explore the generality of Man trimming to M6 and M5, we analyzed the fate of another well known ERAD substrate, unassembled CD3$\delta$, expressed in COS-7 cells. In the absence of other subunits of the T-cell antigen receptor, this protein is retained in the ER and sent to ERAD (16). Longer chase times were used as the degradation in COS-7 cells is slow. The oligosaccharide pattern was similar to that of H2a with a relative increase in M6 and M5 and a decrease of M8 and M9 in the presence of MG-132 (Fig. 3*C*).

When the percent of H2a degraded in pulse-chase experiments was plotted as a function of the abundance of each oligosaccharide species present after the same chase times

[2] Z. Frenkel and G. Z. Lederkremer, unpublished data.

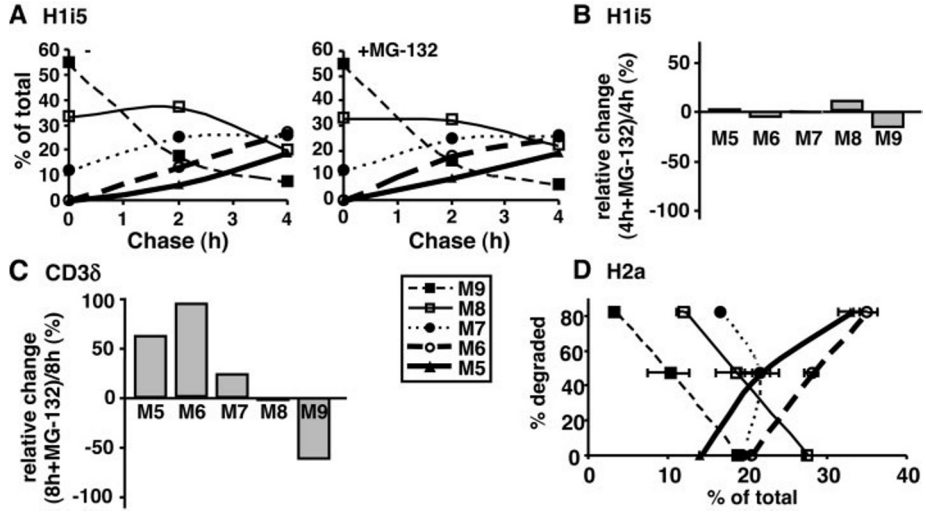


FIG. 3. **Glycoprotein instability and degradation correlate with the extent of Man trimming to M6 and M5.** *A* and *B*, similar to Fig. 1, *C* and *D*, but with NIH 3T3 cells expressing the ASGPR H1 mutant H1i5, ER-retained but very stable as compared with H2a. *C*, similar to Fig. 1*D* but following transiently expressed unassembled CD3δ in COS-7 cells. *D*, phosphorimaging quantitations were done of gels from experiments like those in Fig. 1*A* and Fig. 2*A*. The amount of label remaining in the absence of proteasome inhibitors after different chase times was subtracted from the amount of label that existed after the pulse to obtain the percent degraded. These values were then plotted as a function of the accumulation of the different oligosaccharide species at the same time points but in the presence of proteasomal inhibitors. The values were taken from experiments like those described in Figs. 1*C* and 2*B*.

upon proteasomal inhibition, it was apparent that H2a degradation was inversely proportional to the abundance of M9 and M8 and directly proportional to the abundance of M6 and M5 (Fig. 3*D*). The abundance of M7 did not vary much in relation to the degree of degradation.

*The Last Stages of Transit to the QC Compartment Require Mannose Trimming*—To test the hypothesis that ERAD substrates are targeted to a compartment where the Man trimming takes place, we analyzed the effect of inhibition of dMNJ on the localization of H2a. This inhibitor blocks the degradation of H2a (6), and thus its action should lead to accumulation of H2a at the location where the Man trimming takes place. Upon proteasomal inhibition, H2a accumulated in the QC compartment, represented by a concentrated region close to (but not overlapping with) the Golgi and the ERGIC (Fig. 4). Incubation with dMNJ caused an accumulation of H2a in a similar subcellular location but in a punctate pattern (Fig. 4, *right panels*). This pattern resembles that obtained in real time with an H2a-dsRed fluorescent fusion protein upon proteasomal inhibition for short periods before its entry into the QC compartment.[3] Therefore, inhibition of Man trimming appears to block only the final stages of transit to the QC compartment.

*Trimming to M6 and M5 Terminates the Cycles of Deglucosylation, Reglucosylation, and Calnexin Binding*—After chase, H2a glycans are trimmed to M6 and M5, and no glucosylated peak is discernible (Fig. 1*B*). To analyze whether there is reglucosylation by GT that cannot easily be observed directly because it is followed by fast deglucosylation, the following experiment was performed. Cells expressing H2a were labeled with [$^{35}$S]Cys, and the glucosidase II inhibitor CST was added only during the chase period. In this way, Glc introduced post-translationally by GT cannot be removed, because glucosidase II is blocked. Samples were treated after IP with jack bean α-mannosidase, which, in the absence of a Glc, removes all of the Man residues except for the β-linked core residue (residue *i* in Fig. 5*A*). Indeed, in the absence of CST, H2a glycans were sensitive to the enzyme, which conferred a faster migration (Fig. 5*B*, *lane 5*). The addition of CST caused a slower mobility because of inhibition of trimming of the Glc residue introduced

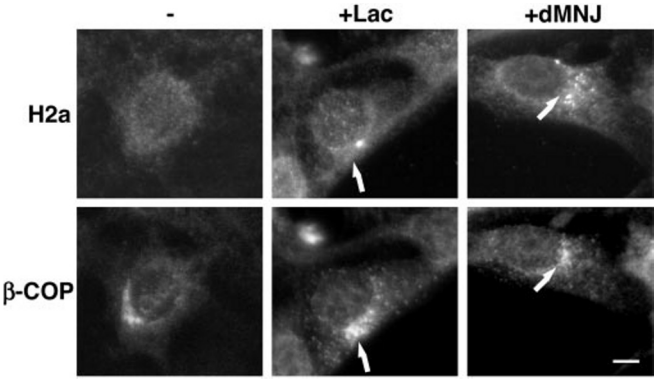


FIG. 4. **Inhibition of Man trimming leads to an accumulation of H2a in a punctate pattern in the region of the QC compartment.** Double-labeled immunofluorescence on fixed and permeabilized cells expressing H2a pre-incubated for 5 h in the absence (*left panels*) or in the presence of 10 μM Lac (*middle panels*) or 75 μg/ml dMNJ (*right panels*). Carboxyl-terminal anti-H2 was used as the primary antibody and Cy3-conjugated goat anti-rabbit IgG as the secondary antibody in the *upper panels*, and mouse monoclonal anti-β-COP with fluorescein isothiocyanate-conjugated goat anti-mouse IgG was used in the *lower panels*. The *arrows* point to the ERGIC and Golgi stained by β-COP, which are near but do not overlap the accumulations of H2a. *Bar*, 10 μm.

by reglucosylation (Fig. 5*B*, compare *lanes 3* and *4*). CST rendered the glycoprotein partially resistant to the α-mannosidase treatment, yielding G1M4 (Fig. 5*B*, *lane 6*) as the Glc residue protects one of the branches of the glycan (Fig. 5*A*). A repeat of the experiment with cells expressing CD3δ gave similar results (Fig. 5*C*). The results suggest efficient reglucosylation followed by deglucosylation of most of the sugar chains before degradation occurs.

We analyzed whether blocking deglucosylation with CST in the chase period can result in an increased binding of H2a to CNX. CNX is seen as being associated with the H2a precursor after a pulse with [$^{35}$S]Cys and to a much lower extent after chase in the absence of CST, although this is partly a result of the reduction in the total amount of H2a because of degradation (Fig. 5*D*). Incubation with CST during the chase led to a significant increase in the fraction of H2a associated to

[3] M. Denisov and G. Z. Lederkremer, unpublished results.

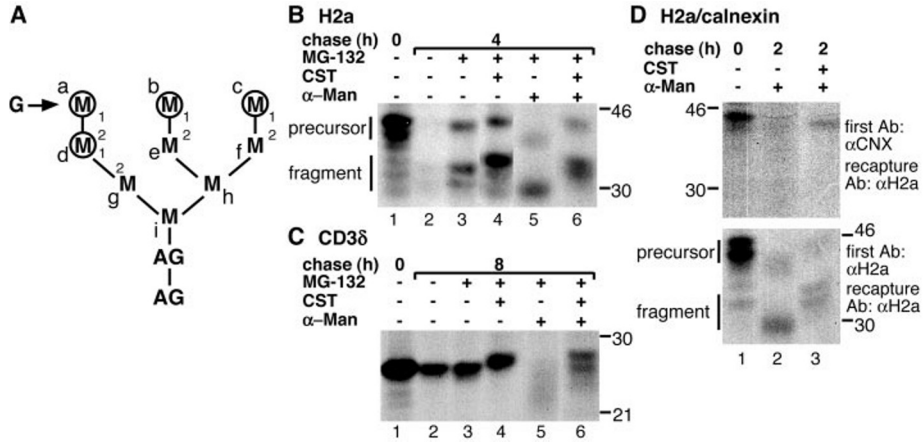


FIG. 5. **The pathway to ERAD involves reglucosylation, CNX binding, deglucosylation, and Man trimming to M6 and M5.** *A*, model of $Man_9GlcNAc_2$ *N*-linked oligosaccharide (M9). *G*, Glc, *M*, Man, *AG*, GlcNAc. The *arrow* after the *G* points to the Man residue where Glc is transferred to by GT. All Man residues with $\alpha$1,2-linkage are *circled*. *a-i* are arbitrary name tags to identify each Man residue. *B*, similar to Fig. 1*A* with the additional treatment of some samples with CST (150 $\mu$g/ml) (present only during the chase period). The indicated samples were treated with jack bean $\alpha$-mannosidase after IP. *C*, similar to *B* but with COS-7 cells transiently expressing CD3$\delta$. *D*, H2a-expressing cells were pulsed with [$^{35}$S]Cys and chased in the absence or presence of 150 $\mu$g/ml CST (present only during the chase period). In the *upper panel*, IP of cell lysates with anti-CNX antibody (*$\alpha$CNX*) was followed by boiling in SDS and re-immunoprecipitation of (*recapture*) with anti-H2a antibody (*$\alpha$H2a*). In the *lower panel,* the first IP was with anti-H2a antibody instead of anti-CNX to analyze total H2a. The indicated samples in both the *upper* and *lower panels* were treated with jack bean $\alpha$-mannosidase after the immunoprecipitation.

CNX (Fig. 5*D*, *upper panel*, *lane 3*). As expected, all of the H2a molecules bound to calnexin were resistant to treatment with jack bean $\alpha$-mannosidase indicating that they were glucosylated.

## DISCUSSION

Our results suggest that the process of ERAD of glycoproteins in mammalian cells involves Man trimming of their *N*-linked sugar chains to render M6 and M5. This was shown for well studied ERAD substrates, ASGPR H2a (a type II membrane protein) and unassembled CD3$\delta$ (a type I membrane protein). A similar fate for a soluble ERAD substrate is suggested by the fact that the same results were obtained with H2a and with an H2a precursor mutant that cannot be cleaved, H2a G78R (12), (Fig. 2*D*). This result points to similar trimming for the soluble 35-kDa fragment derived from H2a, much of which is also targeted to degradation (14). It was also recently reported that for the soluble ERAD substrate HK mutant of $\alpha$1-antitrypsin, some trimming to species smaller than M8 could be seen even in the absence of a proteasomal inhibitor (17).

Man trimming to M5 and M6 was much slower on H1i5, a glycoprotein that is retained in the ER but much more stable toward degradation (Fig. 3, *A* and *B*). Thus, the trimming correlates with degradation and not ER retention. This suggests selective targeting of ERAD substrates for Man trimming. This selectivity could be achieved by targeting these glycoproteins to a compartment where the mannosidase that is responsible for the trimming resides. This possibility is suggested by the accumulation of H2a in a region near the QC compartment upon treatment of cells with dMNJ (Fig. 4). The pattern obtained is similar to that shown by following in real time the fluorescence of an H2a-dsRed fusion protein. Upon proteasomal inhibition, this protein initially moves from the ER to a peripheral punctate pattern. The peripheral dots (possibly vesicular intermediates) then concentrate in the centrosomal region and finally fuse in the QC compartment.[4] Thus, Man trimming seems to be necessary for the last stages of substrate transport to the QC compartment. Because CNX and CRT are also transported to this compartment (10), Man trimming to M6 and M5 would lead to dissociation from the chaperones close to the final destination. This suggests that the Man trimming could act as a timer for rescue attempts that occur on the way to the QC compartment. If these attempts fail, the sugar chains on these ill-fated glycoprotein molecules are trimmed to M6 and M5 leading to proteasomal degradation as depicted in our model (Fig. 6). The fact that GT does not accumulate like CNX and CRT in the QC compartment (10, 18) may suggest recycling of glycoprotein substrates between the bulk of the ER and the QC compartment. Reglucosylation in the ER would lead to CNX binding and traffic toward the compartment, and deglucosylation would allow the molecules to return to the ER for a new round. These cycles would be terminated by Man trimming to M6 and M5. The prediction is that molecules with untrimmed sugar chains will be stable and remain for prolonged periods in the calnexin cycle. In fact, the stable ER-retained H1i5 shows much slower trimming (Fig. 3, *A* and *B*) and very extended association with calnexin (13).

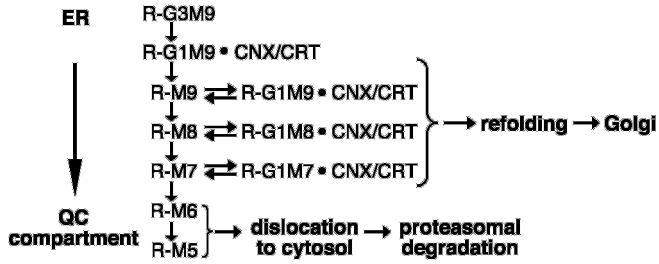


FIG. 6. **Model depicting the processing of *N*-linked oligosaccharides leading to ERAD.** Transfer of the precursor oligosaccharide $Glc_3Man_9GlcNAc_2$ to the protein (*R*) takes place in the ER. Two Glc residues are trimmed, and the glycoprotein then binds CNX or CRT. On the way to the QC compartment, there would be Man trimming to M7 and rescue attempts (refolding) that involve cycles of reglucosylation, CNX binding, and deglucosylation. Release from these cycles could come about by correct protein folding, cleavage, or assembly and exit to the Golgi. For molecules that cannot be rescued, release from the cycles would be accomplished by further Man trimming to M6 and M5 followed by dislocation to the cytosol and proteasomal degradation.

Reports for many ERAD substrate glycoproteins lead to the conclusion that Man trimming is an obligatory step for the degradation to occur (6–8) (reviewed in Ref. 4). Mannosidase inhibitors block the degradation of most glycoproteins, with the

[4] M. Denisov and G. Z. Lederkremer, unpublished results.

notable exception of unassembled T-cell antigen receptor (TCR) $\alpha$ chain (16), a glycoprotein that may behave differently because of two charged residues in its transmembrane domain that may reduce its efficiency as a stop transfer signal (19).

ER mannosidase I has been widely suggested as being responsible for the Man trimming involved in ERAD (4, 7). In *Saccharomyces cerevisiae*, deletion of its sole ER/mannosidase, Mns1p (homologue of mammalian ER mannosidase I) decreased the degradation of an ERAD substrate (20). It was reported recently that, in mammalian cells, overexpression of ER mannosidase I accelerates degradation of an ERAD substrate glycoprotein (17). However, ER mannosidase I acting alone is unlikely to produce M6 and M5. At very high concentrations and after long incubation times, ER mannosidase I can trim up to 4 Man residues *in vitro* (21), but this probably does not occur *in vivo*. A possible candidate for Man trimming leading to ERAD is Man9-mannosidase, which trims M9 to M6 and slowly to M5 (22). Therefore, this enzyme could act alone or in conjunction with ER mannosidase I. The location of Man9-mannosidase was initially reported in the ER (23, 24). However, the enzyme was found to be identical to Golgi mannosidase I A (24, 25), one of three described class I Golgi mannosidases (26) that has a cell type-dependent distribution (27, 28). It is possible that the enzyme cycles through the ER, ERGIC, Golgi, and the QC compartment with a higher steady state abundance in one of these locations depending on the cell type. A similar cycling behavior was described for Golgi glycosyltransferases in yeast (29) and mammalian cells (30).

We propose that the escape from cycles of reglucosylation and CNX binding before delivery to ERAD is the result of trimming to M5 and M6. How is this achieved? Glc is always transferred by GT to the same Man residue (Fig. 5*A,* residue *a*) *in vitro* and *in vivo*.[5] $\alpha$-1,2-Mannosidases would remove a maximum of two terminal Man residues from M9 (Fig. 5*A*, residues *b* and *c*) before removing the one that receives the Glc residue (Fig 5*A*, residue *a*) and effectively blocking reglucosylation. In fact, in the case of H2a, inhibition of trimming of the Glc blocks the trimming of the Man residues of the same branch of the sugar chain causing the molecules to remain bound to CNX (Fig. 5*D*). In contrast to our finding in mammalian cells, in *S. cerevisiae* Man trimming yields M8 (31), which is consistent with a lack of GT and of the reglucosylation/CNX binding cycle in the fission yeast (2). Our model would predict that the main determinant enabling proteasomal degradation to proceed is not the size of the oligosaccharide but the removal of specific Man residues. Indeed, these are the same residues removed in mutant cells that transfer a specific M5 isomer to protein instead of $Glc_3Man_9GlcNAc_2$ (32). This M5 isomer (which contains residues *a*, *d*, *g*, *h*, and *i* (Fig. 5*A*)) can be glucosylated (32), and *in vitro* studies show that the resulting G1M5 is able to bind CNX (33). Before degradation of the glycoprotein, the M5 isomer undergoes trimming of Man residue *a* (Fig. 5*A*), the Glc acceptor.

Future work should explore the roles of M5 and M6 as possible ligands of the putative Man lectin EDEM. Association to EDEM could ensure that after Man trimming and release from CNX, the doomed glycoprotein does not exit to the Golgi. Although the mechanism is not understood, overexpression of EDEM in mammalian cells led to removal of an ERAD substrate from the CNX cycle and to its accelerated degradation, whereas its down-regulation slowed down the degradation (34–36). Perhaps the interaction between EDEM and the glycoproteins takes place through trimmed M5 and M6 sugar chains. Deletion of the *S. cerevisiae* homologue of EDEM also decreased degradation (37). It is conceivable that the yeast homologue may have M8 as its ligand.

*Acknowledgments*—We are grateful to L. Samelson for anti-CD3$\delta$ antibodies and to C. Terhorst for a plasmid for expression of murine CD3$\delta$.

[5] A. J. Parodi, personal communication.

REFERENCES

1. Ellgaard, L., and Helenius, A. (2003) *Nat. Rev. Mol. Cell. Biol.* **4,** 181–191
2. Parodi, A. J. (2000) *Annu. Rev. Biochem.* **69,** 69–93
3. Helenius, A., and Aebi, M. (2001) *Science* **291,** 2364–2369
4. Cabral, C. M., Liu, Y., and Sifers, R. N. (2001) *Trends Biochem. Sci.* **26,** 619–624
5. Liu, Y., Choudhury, P., Cabral, C. M., and Sifers, R. N. (1999) *J. Biol. Chem.* **274,** 5861–5867
6. Ayalon-Soffer, M., Shenkman, M., and Lederkremer, G. Z. (1999) *J. Cell Sci.* **112,** 3309–3318
7. Fagioli, C., and Sitia, R. (2001) *J. Biol. Chem.* **276,** 12885–12892
8. de Virgilio, M., Kitzmuller, C., Schwaiger, E., Klein, M., Kreibich, G., and Ivessa, N. E. (1999) *Mol. Biol. Cell* **10,** 4059–4073
9. Bonifacino, J. S., and Weissman, A. M. (1998) *Annu. Rev. Cell Dev. Biol.* **14,** 19–57
10. Kamhi-Nesher, S., Shenkman, M., Tolchinsky, S., Fromm, S. V., Ehrlich, R., and Lederkremer, G. Z. (2001) *Mol. Biol. Cell* **12,** 1711–1723
11. Lederkremer, G. Z., and Lodish, H. F. (1991) *J. Biol. Chem.* **266,** 1237–1244
12. Yuk, M. H., and Lodish, H. F. (1993) *J. Cell Biol.* **123,** 1735–1749
13. Shenkman, M., Ayalon, M., and Lederkremer, G. Z. (1997) *Proc. Natl. Acad. Sci. U. S. A.* **94,** 11363–11368
14. Tolchinsky, S., Yuk, M. H., Ayalon, M., Lodish, H. F., and Lederkremer, G. Z. (1996) *J. Biol. Chem.* **271,** 14496–14503
15. Mellis, S. J., and Baenziger, J. U. (1981) *Anal. Biochem.* **114,** 276–280
16. Yang, M., Omura, S., Bonifacino, J. S., and Weissman, A. M. (1998) *J. Exp. Med.* **187,** 835–846
17. Hosokawa, N., Tremblay, L. O., You, Z., Herscovics, A., Wada, I., and Nagata, K. (2003) *J. Biol. Chem.*, **278,** 26287–26294
18. Zuber, C., Fan, J. Y., Guhl, B., Parodi, A., Fessler, J. H., Parker, C., and Roth, J. (2001) *Proc. Natl. Acad. Sci. U. S. A.* **98,** 10710–10715
19. Shin, J., Lee, S., and Strominger, J. L. (1993) *Science* **259,** 1901–1904
20. Knop, M., Hauser, N., and Wolf, D. H. (1996) *Yeast* **12,** 1229–1238
21. Herscovics, A., Romero, P. A., and Tremblay, L. O. (2002) *Glycobiology* **12,** 14G–15G.
22. Bause, E., Breuer, W., Schweden, J., Roeser, R., and Geyer, R. (1992) *Eur. J. Biochem.* **208,** 451–457
23. Roth, J., Brada, D., Lackie, P. M., Schweden, J., and Bause, E. (1990) *Eur. J. Cell Biol.* **53,** 131–141
24. Bieberich, E., Treml, K., Volker, C., Rolfs, A., Kalz-Fuller, B., and Bause, E. (1997) *Eur. J. Biochem.* **246,** 681–689
25. Lal, A., Schutzbach, J. S., Forsee, W. T., Neame, P. J., and Moremen, K. W. (1994) *J. Biol. Chem.* **269,** 9872–9881
26. Herscovics, A. (2001) *Biochimie* (*Paris*) **83,** 757–762
27. Velasco, A., Hendricks, L., Moremen, K. W., Tulsiani, D. R., Touster, O., and Farquhar, M. G. (1993) *J. Cell Biol.* **122,** 39–51
28. Igdoura, S. A., Herscovics, A., Lal, A., Moremen, K. W., Morales, C. R., and Hermo, L. (1999) *Eur. J. Cell Biol.* **78,** 441–452
29. Todorow, Z., Spang, A., Carmack, E., Yates, J., and Schekman, R. (2000) *Proc. Natl. Acad. Sci. U. S. A.* **97,** 13643–13648
30. Storrie, B., White, J., Rottger, S., Stelzer, E. H. K., Suganuma, T., and Nilsson, T. (1998) *J. Cell Biol.* **143,** 1505–1521
31. Jakob, C. A., Burda, P., Roth, J., and Aebi, M. (1998) *J. Cell Biol.* **142,** 1223–1233
32. Ermonval, M., Kitzmuller, C., Mir, A. M., Cacan, R., and Ivessa, N. E. (2001) *Glycobiology* **11,** 565–576
33. Vassilakos, A., Michalak, M., Lehrman, M. A., and Williams, D. B. (1998) *Biochemistry* **37,** 3480–3490
34. Oda, Y., Hosokawa, N., Wada, I., and Nagata, K. (2003) *Science* **299,** 1394–1397
35. Hosokawa, N., Wada, I., Hasegawa, K., Yorihuzi, T., Tremblay, L. O., Herscovics, A., and Nagata, K. (2001) *EMBO Rep.* **2,** 415–422
36. Molinari, M., Calanca, V., Galli, C., Lucca, P., and Paganetti, P. (2003) *Science* **299,** 1397–1400
37. Nakatsukasa, K., Nishikawa, S., Hosokawa, N., Nagata, K., and Endo, T. (2001) *J. Biol. Chem.* **276,** 8635–8638